MRS Communications (2015), 5, 447–452

doi:10.1557/mrc.2015.60

MRS Communications

Polymers/Soft Matter Research Letter

Suppressing crystallization in solution-processed thin films of organic semiconductors

Jes B. Sherman, Department of Chemistry and Biochemistry, University of California Santa Barbara, Santa Barbara, CA 93106, USA
Chien-Yang Chiu, and **Ryan Fagenson,** Materials Department, University of California Santa Barbara, Santa Barbara, CA 93106, USA
Guang Wu, Department of Chemistry and Biochemistry, University of California Santa Barbara, Santa Barbara, CA 93106, USA
Craig J. Hawker, Department of Chemistry and Biochemistry, University of California Santa Barbara, Santa Barbara, CA 93106, USA; Materials Department, University of California Santa Barbara, Santa Barbara, CA 93106, USA
Michael L. Chabinyc, Materials Department, University of California Santa Barbara, Santa Barbara, CA 93106, USA

Address all correspondence to Michael L. Chabinyc at **mchabinyc@engineering.ucsb.edu**

(Received 5 June 2015; accepted 27 July 2015)

Abstract

Glassy organic semiconductors provide a convenient host for dispersing guest molecules, such as dopants or light-emitting chromophores. However, many glass-forming compounds will crystallize over time leading to changes in performance and stability in devices. Methods to stabilize amorphous molecular solids are therefore desirable. We demonstrate that solution-processable glasses can be formed from a mixture of 8,8′-biindeno[2,1-*b*]thiophenylene (BTP) atropisomers. While the *trans* isomer of methylated BTP, (*E*)-MeBTP crystallizes in spin-cast films, the addition of (*Z*)-MeBTP slows the growth of the spherulites. X-ray scattering and optical microscopy indicate that films containing 40% (*Z*)-MeBTP do not crystallize, even with the addition of nucleation agents and aging for several months.

Introduction

Producing amorphous organic solids, and preventing their crystallization, presents a challenge in organic electronics, pharmaceutical science, and energetic materials.[1,2] Amorphous materials are required when an application requires features such as maintenance of particular domains sizes over time, a host matrix for molecular species, or a stable dissolution rate of a solid. A difficulty in maintaining a glassy form of an organic solid is crystallization where small crystallites, which are thermodynamically disfavored because of their high relative surface areas, grow over time. This transformation leads to a decline in materials performance for applications that require small-sized particles or phase separated structures with small domain sizes. This need is particularly relevant to organic light emitting diodes (OLEDs). Many high performance OLEDs are formed with an emissive guest in a host material; crystallization of the emitting material can lead to dark areas within a device.[3] Futhermore, organic photovoltaics (OPVs) often suffer deterioration in device performance over time as one or more components in a bulk heterojunction device crystallize, leading to larger aggregates.[4] To prevent the situation, a common solution is to use molecular materials with relatively stable amorphous phases, i.e., molecular glasses.

Intentional design of molecular glasses can be challenging. Because molecular structure has a strong influence on packing in molecular solids, a common strategy to produce glassy organic materials is to add steric hindrance between molecules and conformational flexibility in the molecular structures, thus slowing crystallization.[5,6] This approach has successfully led to high performance hole transport materials, such as spiro-OMeTAD for perovskite and dye-sensitized solar cells.[7–9] Other strategies include synthesis of molecules with high glass transition temperatures (T_g), which extends the range of operating temperatures for devices.[2,10] Structurally similar additives can also be blended with active pharmaceutical ingredients to inhibit crystallization or, in lower concentrations, to alter crystal habit.[11–13] This strategy has rarely been used in organic electronics, but hypereutectics of structurally similar acenes have been used to control crystallization in forming thin film transistors (TFTs),[14] and blends of $PC_{61}BM$ with $PC_{71}BM$ has been shown to suppress fullerene crystallization in bulk heterojunction (BHJ) OPVs.[15,16] Additionally, a hole-transporting indolo[3,2-*b*]carbazole comprising two atropisomers—isolable conformers that differ by sterically hindered rotation about a chemical bond—was shown to form a stable glass with a high T_g (164 °C).[17] Beyond molecular design, processing is also important; exceptionally stable glasses can be formed using vapor deposition by controlling the substrate temperatures and deposition rates.[18]

Here, we produce a highly stable glass by blending a glass-forming compound with its geometric isomer and study the behavior of solution-cast films, which are relevant for printable organic electronic devices. Two geometric isomers of methylated biindene[2,1-b]thiophenylidene ((*E*)- and (*Z*)-MeBTP,

shown in Fig. 1) were used in this study. We show that neat films of the *trans* isomer, (*E*)-MeBTP, slowly crystallize, producing spherulites and dendritic structures within solution cast thin films. However blending (*E*)- with (*Z*)-MeBTP dramatically slows crystallization leading to the formation of stable glasses.

Results and discussion

MeBTP molecules are methylated derivatives of biindene [2,1-b]thiophenylidene (BTP), which contain a twisted central double bond caused by the steric congestion between the proximal aromatic rings. The relief of steric hindrance and the fulfillment of the 14-π-electron rule enable them to readily accept electrons, thus making them alternatives to fullerenes in organic solar cells (OSCs).[19–21] The versatile BTP monomers have also been incorporated into low-bandgap conjugated polymers as donor materials in solar cells.[20] The bulk single crystal structure of (*E*)-MeBTP is shown in Fig. S1. While (*E*)-MeBTP can be purified in large quantity by recrystallization, pure (*Z*)-MeBTP requires chromatographic purification. Therefore, this study focuses on (*E*)-MeBTP, and the mixture of both *trans* and *cis* isomers. Attempts to convert (*E*)-MeBTP to its *cis* isomer by either thermal (heated at 200 °C) or photo-isomerization (using broadband and individual wavelengths in the absorption band) were unsuccessful. Therefore the isomers cannot interconvert readily due to a high barrier to rotation around the central double bond and we can safely assume that there is no significant interconversion of the isomers under the conditions studied.

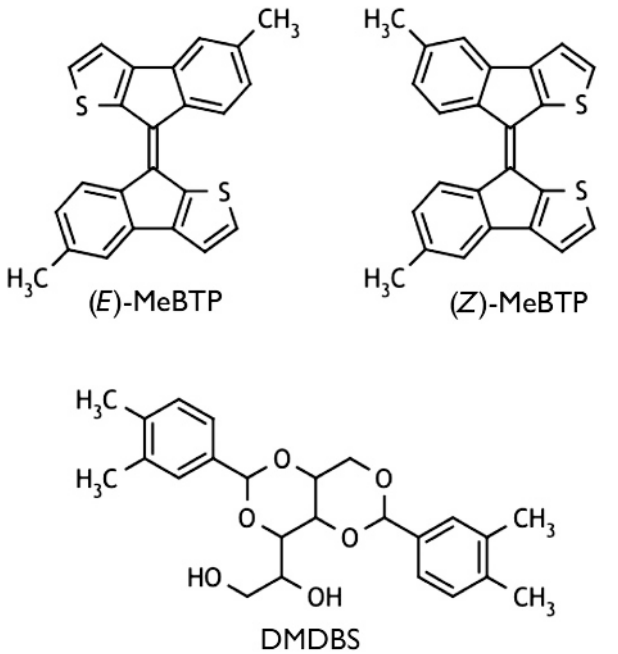

Figure 1. Chemical structures of (*E*)-MeBTP, its isomer (*Z*)-MeBTP, and the nucleation agent DMDBS.

Thermal analysis is useful in determining the stability of glass-forming compounds, and in assessing which temperature ranges favor nucleation and growth. Materials that form stable glasses often do not reveal recrystallization from cooling by differential scanning calorimetry (DSC). This can be attributed to the timescale of the recrystallization process, and to the fact that nucleation does not always take place in the same temperature range as growth.[22] In the case of (*E*)-MeBTP, DSC—performed using a crystalline sample—showed melting only on the first scan, and reproducible glass transitions upon subsequent cooling and reheating to melt (Fig. 2). The absence of crystallization or melting features after several hours of heating/cooling cycles between T_g (337 K) and T_m (473 K) indicates that (*E*)-MeBTP is a stable glass-forming compound. The stability can be quantified by the *reduced* T_g, defined as the ratio T_g/T_m, which is 0.71 for (*E*)-MeBTP; stable glassy materials are believed to have *reduced* T_g of at least 0.66.[23]

It is informative to compare the thermal behavior of (*E*)-MeBTP with a mixture of (*E*)- and (*Z*)-MeBTP isomers. A bulk sample containing a 3:2 mixture of (*E*)- and (*Z*)-MeBTP also shows melting upon first heating, but also fails to show recrystallization or melting upon subsequent heating/cooling cycles (Fig. S2). This failure to recrystallize, as well as the similarity of the glass transition temperatures between (*E*)-MeBTP (T_g = 64 °C) and mixed (*E*)- and (*Z*)-MeBTP (T_g = 64 °C), might seem to indicate that (*E*)-MeBTP isomerizes upon melting, but we discount this possibility because no isomerization was observed when a toluene solution of (*E*)-MeBTP was heated at 200 °C under pressure overnight.

Optical microscopy also reveals that cooling (*E*)-MeBTP from the melt results in a glass, and these bulk samples do

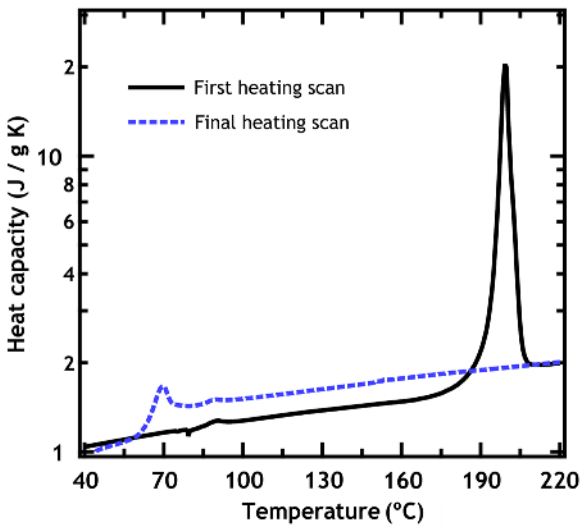

Figure 2. DSC shows melting upon first heating a bulk sample of (*E*)-MeBTP. Despite several heating-cooling cycles in a temperature range thought to promote nucleation and growth, no melting was observed upon reheating to the melting point. This indicates that the material did not crystallize, but a reproducible glass transition at 337 K (64 °C) was observed.

not appear to crystallize upon cooling. An initially-crystalline sample of (*E*)-MeBTP was heated between two microscope cover slips, then cooled to ambient temperature over the course of approximately 1 h, producing a bulk sample approximately 50 µm thick. Crystallization of this sample was not observed by optical microscopy, even after aging for several weeks at ambient temperature. Heating the sample for several hours at 60 °C, a temperature slightly below the T_g, which should favor rapid crystal growth, also yielded no crystallization within 3 weeks of casting. Because diffusion at the surface of molecular glasses is known to facilitate rapid glass-to-crystal growth, we attempted to melt a spincast film of (*E*)-MeBTP, but dewetting of the film was observed at temperatures above 140 °C.[18,24] In order to explore the possibility that surface diffusion might be responsible for crystallization, we prepared an uncovered (*E*)-MeBTP film by melting a sample between two cover slips, and then carefully removing the top cover slip. Optical microscopy revealed no crystallization in this sample, even after aging for 3 weeks at room temperature.

Because solution-processed thin films often display properties differing from bulk samples, we investigated the stability of amorphous MeBTP films produced by spin-casting from solution. Within a few days of spin-casting, spherulites (indicative of crystallization) were evident by optical microscopy of (*E*)-MeBTP films, but not in mixed (3:2) (*E*)- and (*Z*)-MeBTP films (Fig. 3). After aging for several months, neat films of (*E*)-MeBTP were almost entirely covered by spherulite and dendrite growth, with only a small area that still appeared amorphous. By contrast, the mixed films remained nearly completely glassy, with only two small regions of surface crystal growth (less than 50 µm^2 each, in a film of 1.5 cm^2). Atomic force microscopy (AFM) (Fig. 4) shows that the remaining glassy region of the (*E*)-MeBTP film is smooth and similar in texture to the almost entirely glassy mixed film. In an image of the topography by AFM (Fig. 4), a spherulite on the (*E*)-MeBTP film is considerably rougher, but does not show features as tall as a fibrous surface crystal, which reaches more than a micron above the surface. This is similar to previously reported data on organic crystals produced by surface-mediated diffusion.[25]

In an attempt to induce spherulite nucleation and subsequent growth in mixed isomer films, we employed the nucleation agent DMDBS (shown in Fig. 1). DMDBS, 1,3:2,4-di-O-benzylidene-D-sorbitol, has proven effective in inducing nucleation in TIPS-pentacene and semiconducting polymers when cast from solution.[26] When films were cast after a small amount (0.1% by weight) of DMDBS was added to a solution of (*E*)-MeBTP, spherulites were observed to nucleate and grow rapidly; annealing at 60 °C appeared to accelerate this process (Fig. 5). However, the same treatment did not induce any spherulite formation in mixed films containing 3:2 (*E*)-MeBTP:(*Z*)-MeBTP, even after annealing.

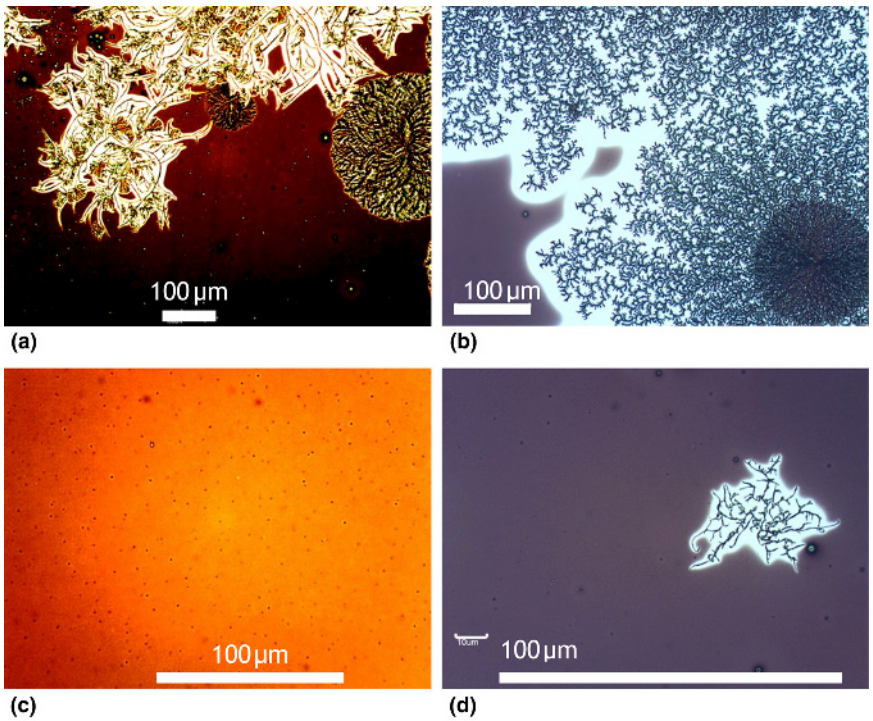

Figure 3. Polarized optical microscope images show spherulite formation in spin-cast films, indicating glass-to-crystal growth, in neat (*E*)-MeBTP films, but not in mixed films containing (*E*)- and (*Z*)-MeBTP. Mixed films only (a) (*E*)-MeBTP, 3 days after casting; (b) (*E*)-MeBTP, 5 months after casting; (c) mixed (*E*)- and (*Z*)-MeBTP, 3 days after casting; (d) mixed (*E*)- and (*Z*)-MeBTP, showing surface crystal growth after 5 months.

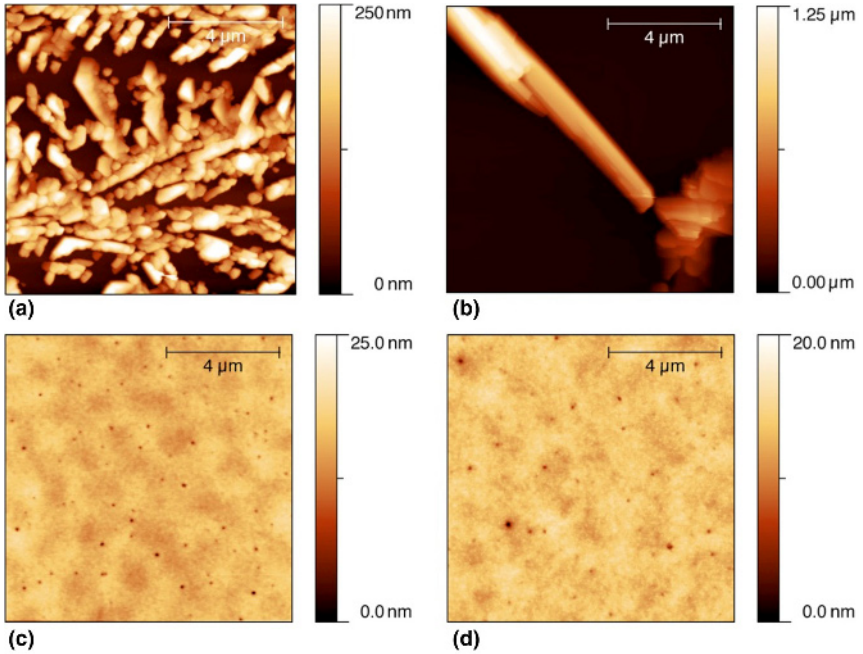

Figure 4. AFM images of spincast films show that (a) a spherulite in a film of (*E*)-MeBTP does not exhibit features as tall as observed for (b) a surface crystal in a film of (*E*)-MeBTP. Transparent regions of (c) a (*E*)-MeBTP film appear identical to (d) the transparent mixed-isomer film.

As optical microscopy can only easily reveal micron scale crystallites in the solution cast films, we also examined whether smaller scale crystallites were present using synchrotron grazing incidence wide angle X-ray scattering (GIWAXS) (Fig. 6). GIWAXS of a thin film (60 nm) of (*E*)-MeBTP shows scattering peaks that match well with data simulated using the bulk structure of the compound (Fig. S3). Because a few peaks are present in the experimental data that do not appear in the simulation data, we believe an additional polymorph of (*E*)-MeBTP is present in the thin films similar to many organic materials. Mixed films containing (*E*)- and (*Z*)-MeBTP, unlike neat (*E*)-MeBTP films, exhibit only a broad amorphous "halo" in GIWAXS. This indicates a lack of crystalline order in the mixed films, even after adding nucleation agents or aging for 6 months, as shown in the optical microscopy (Fig. 5) and the GIWAXS (Fig. 6).

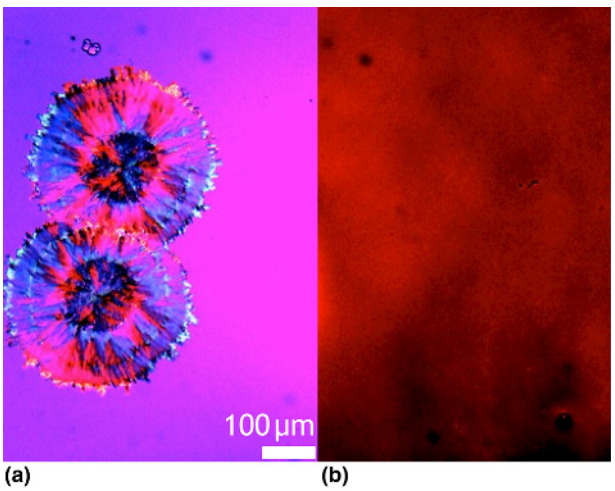

Figure 5. Polarized optical microscope images show that adding nucleation agent DMDBS and annealing for 10 min at 60 °C is sufficient to induce spherulite formation in films of neat (*E*)-MeBTP (left), but not in mixed films containing (*E*)-MeBTP and (*Z*)-MeBTP (right).

Under near-equilibrium growth conditions, structurally similar inhibitors of crystallization attach to kink sites, slowing the step velocity for particular crystal faces.[13,27] This "step-pinning" changes the crystal habit.[12,28] The concentration of inhibitor affects the induction time for crystallization; additive incorporation can induce disorder and broaden reflections.[29] Crystallization in an amorphous thin film differs from near-equilibrium conditions, in that the solvent quickly dries, and then molecules are only free to diffuse across the surface of the film, not through the bulk.[18] We expect that the amount of (*Z*)-MeBTP present should affect the solid-state ordering of (*E*)-MeBTP because, once adsorbed onto the surface of the growing crystals during solvent evaporation, (*Z*)-MeBTP is effectively trapped. Adsorbed (*Z*)-MeBTP prevents the further incorporation of (*E*)-MeBTP at the surface of the crystallites, arresting their growth. This can be inferred from the lack of peak broadening in the GIWAXS data shown in Fig. S4.

Casting films containing different concentrations of (*Z*)-MeBTP reveals that over 20% (*Z*)-MeBTP content is

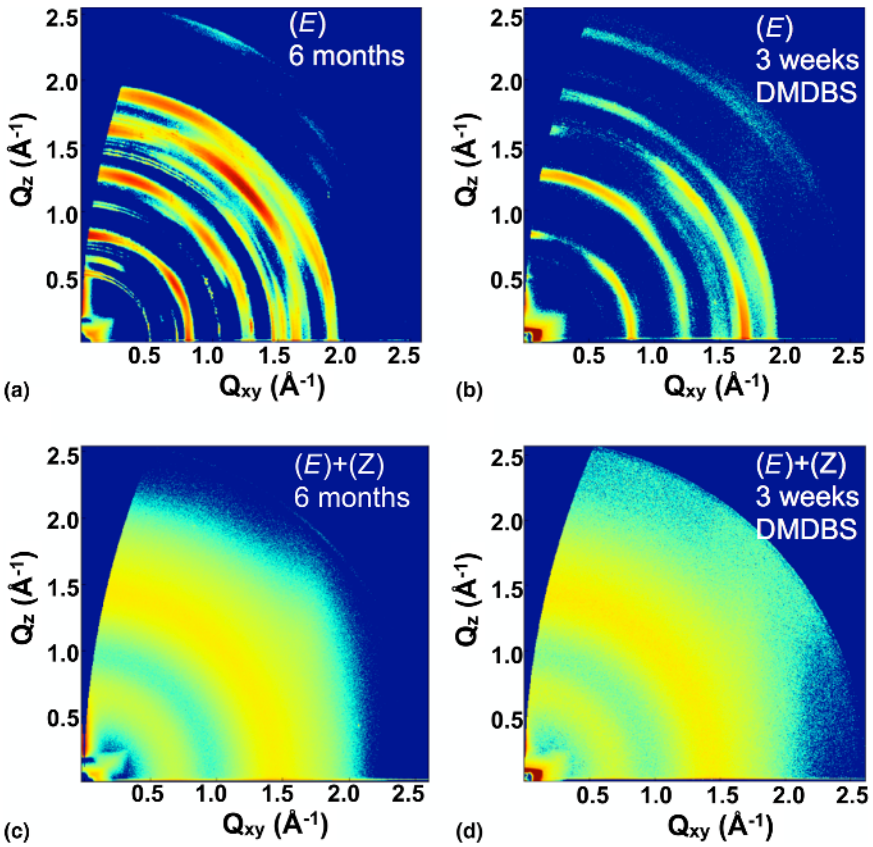

Figure 6. GIWAXS shows neat films of (a) (*E*)-MeBTP and (b) those with the nucleation agent DMDBS show intense scattering peaks. In contrast (c) (3:2) mixed films of (*E*)- and (*Z*)-MeBTP show only a broad amorphous halo, indicating a lack of crystalline order, even after aging for 6 months or (d) with the addition of a nucleation agent.

needed to inhibit growth, as observed by optical microscopy. The film containing 20% (*Z*)-MeBTP exhibited a longer induction time for crystallization—no detectable crystallization had occurred 2 days after casting, but by the 4th day, spherulites were evident. A series of photos, taken over the course of a day using a polarized optical microscope, was used to measure the radius (r) of the spherulites as a function of time (t) and show that films containing less (*Z*)-MeBTP crystallize faster (Fig. S5) The spherulites grow with power law behavior ($r \sim t^n$) where $n \sim 0.5$ for the neat film of (*E*)-MeBTP and $n \sim 0.8$ for the blend films (Fig. S6). The exponent of 0.5 suggests a diffusion process is limiting growth whereas the larger exponent of 0.8 suggests a mixed mechanism involving diffusion and the interface of the crystal.[30] Similar growth behavior has been observed in the conversion of amorphous rubrene to crystalline rubrene formed by vapor deposition.[31]

Conclusion

The stability of organic glasses is important for applications ranging from OLEDs to OPVs making the development of new building blocks that can aid in controlling morphology an important goal. We have shown that (*E*)-MeBTP forms stable glasses from the bulk melt with solution-cast thin films crystallizing slowly. For these solution-cast thin films of (*E*)-MeBTP, glassy areas with pinholes are initially observed and over the course of a few days, sperulites and surface crystals, extending far above the substrate, grow. Low concentrations of (*Z*)-MeBTP retard crystallization of its geometric isomer (*E*)-MeBTP, whereas high concentrations (40%) of (*Z*)-MeBTP appear to stop crystallization altogether. Because (*Z*)-MeBTP does not disrupt the solid-state ordering of (*E*)-MeBTP, we conclude that surface adsorption of (*Z*)-MeBTP arrests crystallite growth. We see a significant increase in the induction time for crystallization upon incorporating 20% (*Z*)-MeBTP within the film. Interestingly, incorporating 15%–20% $PC_{71}BM$ into $PC_{61}BM$ films also leads to suppression of crystallization.[15,16] Random close packed spheres have a nearest neighbor coordination of ~6,[32] suggesting that the observed weight fraction can be rationalized by a need to replace ~1/6 molecules to frustrate crystallization. While the mechanism of inhibition of crystallization likely depends on specific molecular interactions, the comparison of these results suggests that similar ratios should be examined by those seeking to inhibit crystallization in organic blends.

Supplementary materials

For supplementary material for this article, please visit http://dx.doi.org/10.1557/mrc.2015.60

Acknowledgments

J. S and M. L. C were supported by NSF DMR award 1410438. This work made use of MRL Central Facilities supported by the MRSEC Program of the National Science Foundation under award No. DMR 1121053. Use of the Stanford Synchrotron Radiation Lightsource, SLAC National Accelerator Laboratory, is supported by the U.S. Department of Energy, Office of Science, Office of Basic Energy Sciences under Contract No. DE-AC02-76SF00515.

References

1. N.S. Trasi and L.S. Taylor: Effect of polymers on nucleation and crystal growth of amorphous acetaminophen. *CrystEngComm*. **14**, 5188–5197 (2012).
2. M.D. Ediger: Vapor-deposited glasses provide clearer view of two-level systems. *Proc. Natl. Acad. Sci*. **111**, 11232–11233 (2014).
3. H. Aziz, Z. Popovic, S. Xie, A.-M. Hor, N.-X. Hu, C. Tripp, and G. Xu: Humidity-induced crystallization of tris (8-hydroxyquinoline) aluminum layers in organic light-emitting devices. *Appl. Phys. Lett*. **72**, 756–758 (1998).
4. F.C. Krebs: *Stability and Degradation of Organic and Polymer Solar Cells* (John Wiley & Sons, Hoboken, NJ, 2012).
5. Y. Shirota: Photo- and electroactive amorphous molecular materials—molecular design, syntheses, reactions, properties, and applications. *J. Mater. Chem*. **15**, 75–93 (2005).
6. K. Naito and A. Miura: Molecular design for nonpolymeric organic dye glasses with thermal stability: relations between thermodynamic parameters and amorphous properties. *J. Phys. Chem*. **97**, 6240–6248 (1993).
7. F. Fabregat-Santiago, J. Bisquert, L. Cevey, P. Chen, M. Wang, S. M. Zakeeruddin, and M. Grätzel: Electron transport and recombination in solid-state dye solar cell with spiro-OMeTAD as hole conductor. *J. Am. Chem. Soc*. **131**, 558–562 (2009).
8. N.J. Jeon, H.G. Lee, Y.C. Kim, J. Seo, J.H. Noh, J. Lee, and S.I. Seok: o-Methoxy substituents in spiro-OMeTAD for efficient inorganic–organic hybrid Perovskite solar cells. *J. Am. Chem. Soc*. **136**, 7837–7840 (2014).
9. T. Leijtens, I.-K. Ding, T. Giovenzana, J.T. Bloking, M.D. McGehee, and A. Sellinger: Hole transport materials with low glass transition temperatures and high solubility for application in solid-state dye-sensitized solar cells. *ACS Nano* **6**, 1455–1462 (2012).
10. D. Redinger, R.S. Clough, J.C. Novack, G. Caldwell, M.M. Payne, and J. E. Anthony: Novel silylethynyl substituted pentacenes with high-temperature thermal transitions. *MRS Online Proc. Libr*. **1270**, II09–16 (2010).
11. J.D. Rimer, Z. An, Z. Zhu, M.H. Lee, D.S. Goldfarb, J.A. Wesson, and M. D. Ward: Crystal growth inhibitors for the prevention of l-cystine kidney stones through molecular design. *Science* **330**, 337–341 (2010).
12. Z.B. Kuvadia and M.F. Doherty: Effect of structurally similar additives on crystal habit of organic molecular crystals at low supersaturation. *Cryst. Growth Des*. **13**, 1412–1428 (2013).
13. J.P. Sizemore and M.F. Doherty: A new model for the effect of molecular imposters on the shape of faceted molecular crystals. *Cryst. Growth Des*. **9**, 2637–2645 (2009).
14. N. Stingelin-Stutzmann, E. Smits, H. Wondergem, C. Tanase, P. Blom, P. Smith, and D. de Leeuw: Organic thin-film electronics from vitreous solution-processed rubrene hypereutectics. *Nat. Mater*. **4**, 601–606 (2005).
15. C. Lindqvist, J. Bergqvist, O. Bäcke, S. Gustafsson, E. Wang, E. Olsson, O. Inganäs, M.R. Andersson, and C. Müller: Fullerene mixtures enhance the thermal stability of a non-crystalline polymer solar cell blend. *Appl. Phys. Lett*. **104**, 153301 (2014).
16. Y. Santo, I. Jeon, K.S. Yeo, T. Nakagawa, and Y. Matsuo: Mixture of [60] and [70] PCBM giving morphological stability in organic solar cells. *Appl. Phys. Lett*. **103**, 073306 (2013).
17. N.-X. Hu, S. Xie, Z. Popovic, B. Ong, A.-M. Hor, and S. Wang: 5,11-dihydro-5,11-di-1-naphthylindolo[3,2- *b*] carbazole: atropisomerism in a novel hole-transport molecule for organic light-emitting diodes. *J. Am. Chem. Soc*. **121**, 5097–5098 (1999).
18. S.F. Swallen, K.L. Kearns, M.K. Mapes, Y.S. Kim, R.J. McMahon, M. D. Ediger, T. Wu, L. Yu, and S. Satija: Organic glasses with exceptional thermodynamic and kinetic stability. *Science* **315**, 353–356 (2007).
19. F.G. Brunetti, X. Gong, M. Tong, A.J. Heeger, and F. Wudl: Strain and hückel aromaticity: driving forces for a promising new generation of electron acceptors in organic electronics. *Angew. Chem. Int. Ed*. **49**, 532–536 (2010).
20. C.-Y. Chiu, H. Wang, F.G. Brunetti, F. Wudl, and C.J. Hawker: Twisted but conjugated: building blocks for low bandgap polymers. *Angew. Chem. Int. Ed*. **53**, 3996–4000 (2014).
21. X. Gong, M. Tong, F.G. Brunetti, J. Seo, Y. Sun, D. Moses, F. Wudl, and A.J. Heeger: Bulk heterojunction solar cells with large open-circuit voltage: electron transfer with small donor-acceptor energy offset. *Adv. Mater*. **23**, 2272–2277 (2011).
22. J.A. Baird, B. Van Eerdenbrugh, and L.S. Taylor: A classification system to assess the crystallization tendency of organic molecules from undercooled melts. *J. Pharm. Sci*. **99**, 3787–3806 (2010).
23. W. Ping, D. Paraska, R. Baker, P. Harrowell, and C.A. Angell: Molecular engineering of the glass transition: glass-forming ability across a homologous series of cyclic stilbenes. *J. Phys. Chem. B* **115**, 4696–4702 (2011).
24. Y. Sun, H. Xi, S. Chen, M.D. Ediger, and L. Yu: Crystallization near glass transition: transition from diffusion-controlled to diffusionless crystal growth studied with seven polymorphs. *J. Phys. Chem. B* **112**, 5594–5601 (2008).
25. Y. Sun, L. Zhu, K.L. Kearns, M.D. Ediger, and L. Yu: Glasses crystallize rapidly at free surfaces by growing crystals upward. *Proc. Natl. Acad. Sci*. **108**, 5990–5995 (2011).
26. N.D. Treat, J.A. Nekuda Malik, O. Reid, L. Yu, C.G. Shuttle, G. Rumbles, C. J. Hawker, M.L. Chabinyc, P. Smith, and N. Stingelin: Microstructure formation in molecular and polymer semiconductors assisted by nucleation agents. *Nat. Mater*. **12**, 628–633 (2013).
27. A.S. Michaels and F.W. Tausch: Modification of growth rate and habit of adipic acid crystals with surfactants. *J. Phys. Chem*. **65**, 1730–1737 (1961).
28. R.J. Davey, S.N. Black, D. Logan, S.J. Maginn, J.E. Fairbrother, and D.J. W. Grant: Structural and kinetic features of crystal growth inhibition: adipic acid growing in the presence of n-alkanoic acids. *J. Chem. Soc. Faraday Trans*. **88**, 3461–3466 (1992).
29. I. Solomonov, M. Osipova, Y. Feldman, C. Baehtz, K. Kjaer, I.K. Robinson, G.T. Webster, D. McNaughton, B.R. Wood, I. Weissbuch, and L. Leiserowitz: Crystal nucleation, growth, and morphology of the synthetic malaria pigment β-hematin and the effect thereon by quinoline additives: the malaria pigment as a target of various antimalarial drugs. *J. Am. Chem. Soc*. **129**, 2615–2627 (2007).
30. A.G. Shtukenberg, Y.O. Punin, E. Gunn, and B. Kahr: Spherulites. *Chem. Rev*. **112**, 1805–1838 (2012).
31. S.-W. Park, J.-M. Choi, K.H. Lee, H.W. Yeom, S. Im, and Y.K. Lee: Amorphous-to-crystalline phase transformation of thin film rubrene. *J. Phys. Chem. B* **114**, 5661–5665 (2010).
32. G.D. Scott and D.M. Kilgour: The density of random close packing of spheres. *J. Phys. Appl. Phys*. **2**, 863–866 (1969).